eISSN: 2477-7994

JMECS (Journal of Measurements, Electronics, Communications, and Systems)

Vol.00, No.1, Pg.00-00, December 2023

Analysis of Spatio-temporal $PM_{2.5}$ and CO_2 Concentrations Distribution with PSCF and CWT Methods in the Greater Bandung Air Basin

A. S. Adiwidya[1], R. M. Aziz[1], M. B. Afryan[1], T. C. Alexandra[1], M. G. Permadi[1], N. R. Jannah[1], D. R. Amalia[1], N. P. M. Sopian[1], V. Lee[1], R. A. Salam[1] and I. Chandra[1*]

[1] *School of Electrical Engineering, Telkom University, Bandung, 40287, Indonesia*

[*] *indrachandra@telkomuniversity.ac.id*

Manuscript received Month1 19, 2022; revised Month2 10, 2022; accepted Month3 2, 2022 .

The manuscript received, revised and accepted dates will be checked and corrected by the journal office.

Abstract

The limitations of expensive main monitoring stations can be addressed by using low-cost sensor-based measuring stations. A low-cost sensor-based air quality monitoring system has been implemented in Telkom University, BRIN Pasteur, and BRIN Taman Sari areas to measure $PM_{2.5}$ and CO_2 concentration in Bandung vertically and horizontally. Vertically, the CO_2 concentration at the highest measuring station is indirectly affected by local activities. However, $PM_{2.5}$ concentration is still influenced by local actions. Horizontally, using the independent T-test and ANOVA, $PM_{2.5}$ concentrations tended to be homogeneous regarding the significance values in the four periods, namely 0.916, 0.03, 0.727, and 0.047. Meanwhile, the concentration of CO_2 at each station tends to be heterogeneous along significance values of 0.646, 0.03, 0.02, and 0.01. The vertical and horizontal analysis shows that CO_2 concentrations tend to be heterogeneous due to differences in altitude and spatial characteristics of the measurement sites. Meanwhile, $PM_{2.5}$ tends to be more homogeneous by having the same pattern at different heights and spatial locations. The long-distance potential sources of $PM_{2.5}$ are estimated to come from the Indian Ocean and Cirebon region because they have the highest PSCF and CWT values, 0.5-0.7 and 55-65 μg/m^3.

Keywords: Backward trajectory; CO_2; Low-cost sensors; $PM_{2.5}$; PSCF.

DOI: 10.0000/0000000 The DOI number will be assigned when the camera-ready manuscript is available.

1. Introduction

Despite economic progress and technological development, a significant problem that persists is air pollution, which poses a substantial global health risk. Clean air is essential for human well-being and health [1]. According to Government Regulation No. 22 of 2021, "air pollution is the entry or inclusion of substances, energy, and other components into ambient air by human activities so that it exceeds the ambient air quality standard that has been determined" [2]. Meanwhile, in 2018, Indonesia ranked 6th globally in population deaths due to air pollution, with 95,156 reported by the World Health Organization (WHO) [3]. This situation is possible because Indonesia is the fourth most populated globally.

Bandung, one of Indonesia's largest cities, faces a high susceptibility to air pollution. A study conducted by the National Nuclear Energy Agency (BATAN) noted that in 2005-2012 the average annual Particulate Matter with a diameter of 2.5 μm or smaller ($PM_{2.5}$) concentrations in Bandung was 18.55 μg/m^3, which was higher than the annual Indonesian national air quality standard limit for $PM_{2.5}$ (15 μg/m^3) [4]. This circumstance is due to the high population in Bandung (almost 2.5 million people were recorded in 2016, according to the West Java provincial website [5]),

which allows many anthropogenic activities that can cause pollution. In addition, in 2018, the number of large and medium industries reached more than 1000, and the number of potential motorized vehicles reached more than 1.7 million [6].

Geographical factors and sources of pollution outside the city of Bandung can also influence the air pollution problem in the city. Geographically, the city of Bandung is surrounded by mountains and is at an altitude of ±768 m above sea level. The topography of the Bandung area resembles a basin, which presents a challenge for pollutant dispersion due to the highlands causing winds to blow in the opposite direction. Thus, the pollution will be trapped in the basin due to the rotation of the wind. Furthermore, local pollutant concentrations in the Bandung City area are also influenced by long-distance pollutant transportation due to mountain-valley winds and sea-land winds. This problem also causes the deposition of pollutants in the Bandung City area due to changes in the planetary boundary layer (PBL), which depends on air stability and surface temperature.

The existence of an air quality measurement station is essential. However, the price of reference monitoring stations is relatively high, around 10 to 100 thousand USD [7], so installing them in many locations is impossible. One solution is to use a low-cost sensor that costs less than 1000 USD to provide an overview of air quality. A low-cost sensor-based air quality monitoring system was created and has been well calibrated according to standard one for measuring the distribution of pollution in the Bandung area. The data obtained through this system will later be used to determine the characteristics of $PM_{2.5}$ and Carbon Dioxide (CO_2) due to the influence of local activities in different locations vertically and horizontally and from which indications of long-distance pollution sources are indicated. In this study, the air quality monitoring system was equipped with six parameters, namely, $PM_{2.5}$, CO_2, Temperature (T), Relative Humidity (RH), light intensity, and air pressure. Each measuring station is placed on top of the building at different heights. Prior to measurement, each sensor must undergo calibration to align its readings with the main instrument. Once measurements are taken, the data is transmitted to the cloud server. Then the data will be analyzed using three points of view, reviewed vertically and horizontally, as well as the potential for long-distance pollution using a backward trajectory.

2. Research Method

2.1 Location and Time of Measurement

Measurements were conducted at five stations in Bandung from April 21 to August 04, 2022. There are three measuring stations above the Telkom University lecture building: the Deli Building, the General Lecture Building (GKU), and the Telkom University Landmark Tower (TULT). The height of each building varies, that is, the Deli building (~15 m), GKU (~35 m), and TULT (~70 m). In addition, there are also two more measuring stations located respectively at the National Research and Innovation Agency (BRIN) Pasteur and BRIN Taman Sari. The two measuring stations are approximately 10 km away from Telkom University, while the distance between the two stations is only around 2 km. It can be seen in Fig. 1 measuring station shelters at 5 locations.

Fig. 1. Shelter station measuring at: (a) Deli, (b) GKU, (c) TULT, (d) BRIN Pasteur, and (e) BRIN Taman Sari.

The secondary data is in the form of Wind Speed (WS) and Wind Direction (WD) from the Meteorology, Climatology, and Geophysics Agency (BMKG) station [8] and BRIN Taman Sari. The distances between Telkom University and the Geophysics station and between Telkom University and the Taman Sari station are approximately 13 km and 10 km, respectively. The daily average T and RH are almost the same at the Telkom University measuring station and the Geophysics station in the range of 20-33°C and 49-95%. Because the two stations are also located in the same topography, namely the Bandung basin area, it can be assumed that both locations have the same air mass so that the wind direction and speed are also relatively the same [9], as well as Taman Sari station which is only ±2km from the station Geophysics.

All measurements were taken on tall buildings to account for intense solar radiation, which leads to increased photochemical activity and significant diurnal temperature variations at higher altitudes. Photochemical models play a crucial role in

evaluating and examining the behavior of atmospheric trace gases and dust particles in a specific area [10]. Even in tropical and subtropical climate zones, temperatures are lower than at sea level for the same latitudes. In addition, the RH at various elevations during the day depends on T and cloud formation. However, the same RH will be achieved at higher altitudes because it contains less water vapor. Previous research [11] stated that RH, which is affected by the elevation of sites, has a positive correlation with $PM_{2.5}$ measurements, therefore the elevation of the measurement site is an aspect that affects the quality of the data obtained. Multiple studies have concluded that elevated RH levels diminish urban $PM_{2.5}$ pollution [12–16].

2.2 Low-cost sensor-based measuring instrument

Prior to measurement, calibrating each sensor is essential to align its values closely with the main instrument or establish a consistent data trend. Low-cost sensors must be validated and calibrated regularly to obtain the best sensor accuracy. Both sensors have been validated one step ahead of previous studies. For the $PM_{2.5}$ sensor, the working principle is to use light scattering. The sensor emits a specific volume of infrared light over a defined distance to the photodetector. The photodetector then measures the amount of light it receives, and this intensity is used to determine particle mass concentration [17]. Besides, the CO_2 sensor uses the non-dispersive infrared (NDIR) principle to detect the presence of CO_2 in the air. This non-dispersive method is a spectroscopy method commonly used to detect gases called non-dispersive because this method passes all infrared wavelengths with a certain intensity through the sample tube without deformation. A non-dispersive infrared sensor comprises three key components: an infrared source, a sample tube, and an infrared detector, as illustrated in NDIR diagrams [18].

Because the main instrument for measuring $PM_{2.5}$ concentrations was not yet available, a comparative test was carried out by attaching sensors from each measuring station to measure $PM_{2.5}$ concentrations. Due to device limitations, sensor comparisons cannot be performed all in parallel. In Fig. 2, the results of the comparison between the $PM_{2.5}$ sensors of the Deli, GKU, and TULT measuring stations have almost the same values. However, there is still a considerable gap at high concentrations above 100 $\mu g/m^3$. For concentrations below 100 $\mu g/m^3$, the gap between the three sensors is only about ±20 $\mu g/m^3$ with a lag time of ±120 seconds, according to the delay during data collection. Then, for the $PM_{2.5}$ sensor comparison test at the Pasteur and Taman Sari measuring stations, the GKU sensor was taken as a comparison for each measuring station, seen in Fig. 3 results of a comparative test between the $PM_{2.5}$ sensor at the GKU measuring station with the $PM_{2.5}$ sensor at the Pasteur and Taman Sari measuring stations and obtained data trends that are almost the same as the standard deviation of 8-13.3 $\mu g/m^3$.

The CO_2 sensor calibration uses the same main instrument, the CO_2 Analyzer. Measurements were made in a test chamber injected with CO_2 gas. In Fig. 4, it can be seen that the Deli sensor response to the main instrument is quite good in the 1000-1500 parts per million (ppm) measurement range, however, a notable gap becomes evident at higher concentrations. Meanwhile, the GKU and TULT sensor responses tend to be homogeneous, but there is still a large gap of around ±500 ppm because they are carried out at high concentrations of up to ±6000 ppm. The data is quite tolerable from the datasheet because the sensor accuracy value is ±(50 ppm + 5% sensor readings). Then, it can be seen in Fig. 5 that CO_2 sensors Pasteur and Taman Sari have a reasonably homogeneous data trend with the main instrument with a standard deviation of 49-69 ppm.

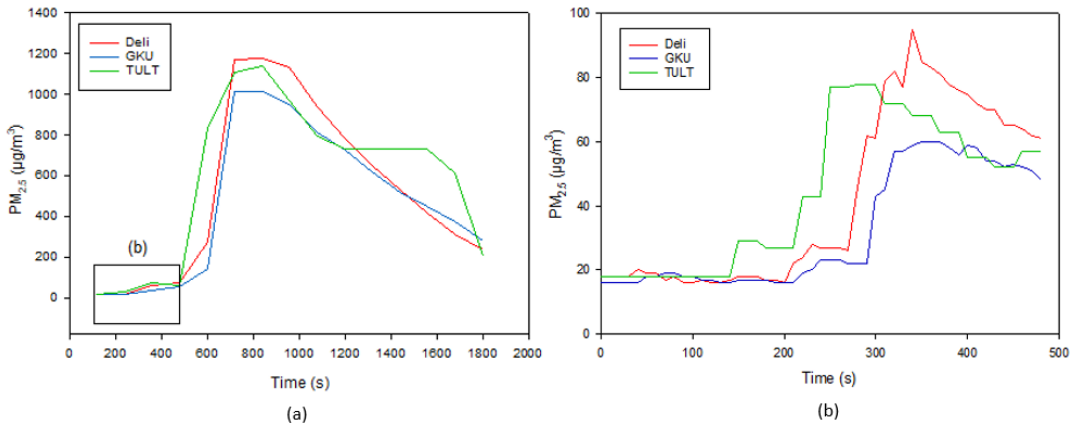

Fig. 2. Comparison graph of three $PM_{2.5}$ sensors: Deli, GKU, and TULT: (a) in range 0 to 1200 µg/m^3 and (b) in range 0 to 100 µg/m^3.

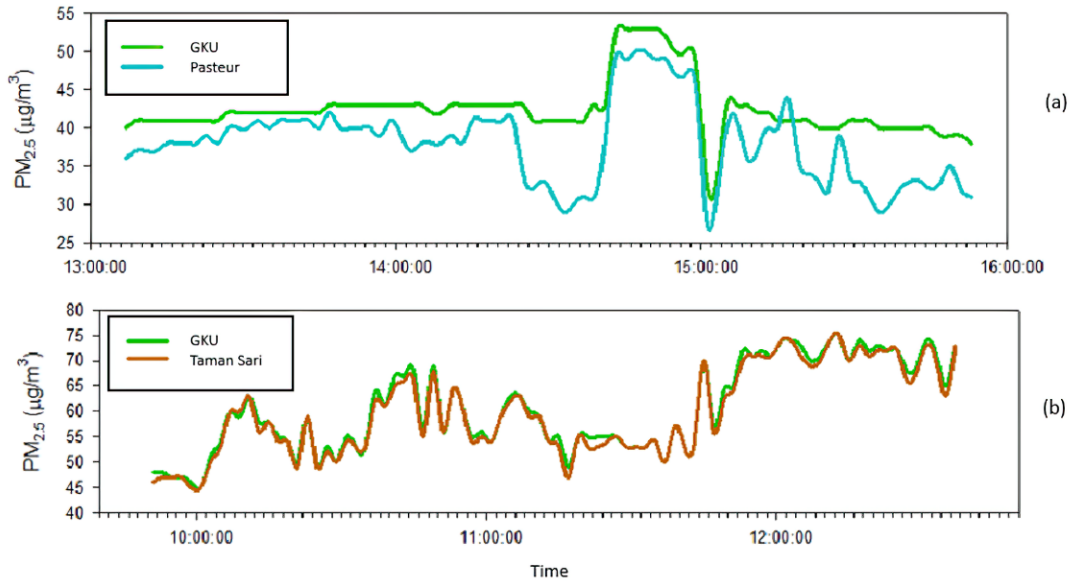

Fig. 3. Comparison graph of (a) GKU with Pasteur $PM_{2.5}$ sensors and (b) GKU with Taman Sari $PM_{2.5}$ sensors.

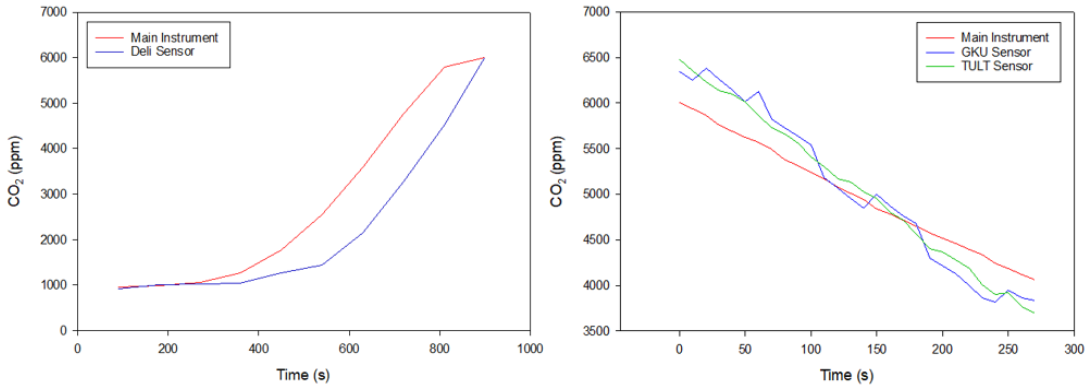

Fig. 4. Calibration graph: (a) is Deli CO_2 Sensor with main instrument and (b) is GKU and TULT CO_2 Sensor with main instrument.

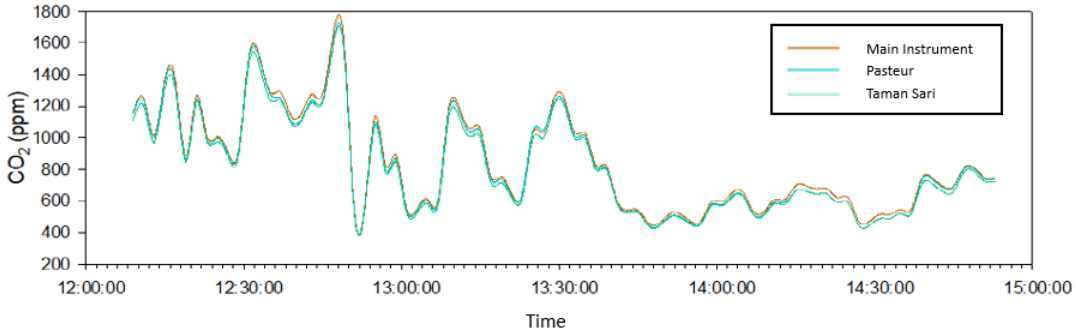

Fig. 5. Calibration graph of Pasteur and Taman Sari CO_2 Sensor with main instrument.

Each measuring station has six parameters, which are $PM_{2.5}$, CO_2, T, RH, light intensity, and air pressure. Data from these sensors is then read and transmitted using an Espressif 32 (ESP32) connected to Wi-Fi. The online data is sent to the Antares cloud server for each measuring station. Before the online system is operational, data storage is done offline using the Arduino Uno microcontroller and data logger. The online modem system design is subsequently transmitted to the cloud server. Data from the cloud server can be downloaded, and then validated on $PM_{2.5}$ and CO_2 parameters. The $PM_{2.5}$ sensor is overestimated when the RH is 80%. Hence, under these conditions, the measured data must be multiplied by a correction factor of 0.67 to obtain valid data [19]. In addition, the $PM_{2.5}$ concentration value must also be in the sensor reading range of 0-999 $\mu g/m^3$. The outliers are removed to validate CO_2 concentration using quartiles 1 and 3 with a 0-5000 ppm measurement range.

2.3 Independent T-test / one-way analysis of variance (ANOVA)

One-way Analysis of Variance (ANOVA) is a statistical method that concludes whether the mean values of two or more groups differ. This method uses a probability distribution to measure the variance. In ANOVA, a significant p-value indicates at least one pair of groups with a statistically significant mean difference [20]. The significance level is the probability of rejecting the null hypothesis when it is true [21]. If the value of the significance level is more than 0.05, it means that two or more groups are correlated and can be called homogeneous. Similar to the previous study, the ANOVA test results support evidence of homogeneity among the selected countries in investigating the relationship between environmental pollution, terrorism, foreign direct investment (FDI), energy consumption, and economic growth [22]. Conversely, if the significance value is less than 0.05, it means that two or more groups are not correlated and can be called heterogeneous.

2.4 Potential Source Contribution Factor (PSCF) and Concentration-Weight Trajectory (CWT) Method

The Potential Source Contribution Factor is a method for determining pollutant source areas based on air parcel trajectories [23]. This method has been widely used to identify potential sources of a pollutant [24–26]. It can be applied if data has been obtained from the concentration of a pollutant to be analyzed and backward vector data for the analyzed period. PSCF value can be obtained by using the formula:

$$PSCF_{ij} = \frac{m_{ij}}{n_{ij}} \quad (1)$$

$PSCF_{ij}$ is the probability of source area on grid cell ij (Coordinate of grid cell), m_{ij} is the total pollutant path points on grid ij, and n_{ij} is the total trajectory points on grid ij.

Several studies have also presented the Concentraiton-Weight Trajectory as a complement to PSCF [24–26]. One of the limitations of the PSCF method is that the results depend on the criterion value of pollutant concentration, so concentration values that are high and much higher than the threshold are not distinguished. CWT_{ij} also uses grid cells where the average concentration of each grid cell is then calculated based on the passing trajectory and the settling time. Based on the formula:

$$CWT_{ij} = \frac{1}{\sum_{l=1}^{M} \tau_{ijl}} \sum_{l=1}^{M} c_l \tau_{ijl} \quad (2)$$

Where M is the total number of routes, l is the track index, τ_{ij} is the air parcel settling time based on the path points on grid ij, and c_l is the pollutant concentration when the path passes through grid ij. The CWT value illustrates the contribution from the potential pollutant source area. Similar to the PSCF, the final results of the CWT will also be shown in map form. Areas with high CWT values indicate a high contribution to the measured concentration value at the receptor [23].

3. Result and Discussion

The discussion uses three points of view: vertically, horizontally, and the potential for long-distance pollution using a backward trajectory.

3.1 Vertical Analysis

The vertical review was carried out using diurnal variation analysis by observing the hourly frequency to see when the fluctuations in pollution occurred [27]. The characteristics of the data on an hourly basis can be seen by counting an hourly average of $PM_{2.5}$ and CO_2 concentrations for each day during the measurement time. Additionally, the data were classified on weekdays and weekends to know the effect of community activities on the concentration of $PM_{2.5}$ and CO_2. For vertical analysis, data from three measuring stations with different heights were carried out, namely the Deli building (~15 m), GKU (~35 m), and TULT (~70 m). From Fig. 6, it can be seen that the CO_2 concentration at the TULT measuring station tends to be lower than at the GKU and Deli measuring stations. This is because, at an altitude of fewer than 300 m, the negative correlation between CO_2 and altitude will be very high, especially at an altitude of less than 100 m [28]. As seen on several days, a lower concentration of CO_2 in GKU during the day compared to Deli could be caused by wind speed. During the day, the wind speed is relatively faster, especially at higher altitudes. In addition, it can be seen that for CO_2 concentrations on weekdays and weekends, there is no significant difference, especially for TULT measuring stations whose data trends are relatively more stable with relative concentrations at 450 - 500 ppm compared to the other two measuring sites, which are affected by changes in day and night activities. This indicates that local activities that produce CO_2 gas do not directly affect this measuring station.

For $PM_{2.5}$ concentrations on weekdays and weekends, Fig. 7 shows that on weekends $PM_{2.5}$ concentrations at Deli and GKU measuring stations tend to be higher than on weekdays, so it is necessary to review the distribution of days during weekends. However, the opposite happened at the TULT measuring station, and this indicates that the source of $PM_{2.5}$ pollutant that has the most influence on the TULT building is on weekdays which can be caused by the activities of returning and going to work in the community or routine waste burning activities. In addition, the concentration of $PM_{2.5}$ at the TULT measuring station was less affected by a decrease in PBL at night, in contrast to the other two stations, which showed an increase in $PM_{2.5}$ concentration at night due to a decrease in PBL. As seen in Fig. 8, there is an increase in GKU and TULT measuring stations from morning to afternoon on Sundays. This may be due to the activities of the Sunday morning market, which is often visited by the public. However, this phenomenon has little effect on the Deli measuring station, perhaps due to the wind direction in the morning, which mostly blows towards the Northwest, while the location of the Deli building is further south than the other two measuring stations. In addition, the two measuring stations are also higher so that the air coverage is broader, in contrast to the Deli measuring station, which is only ±15m high. In addition, there is no indication of an inversion layer because the temperature gradient tends to be negative.

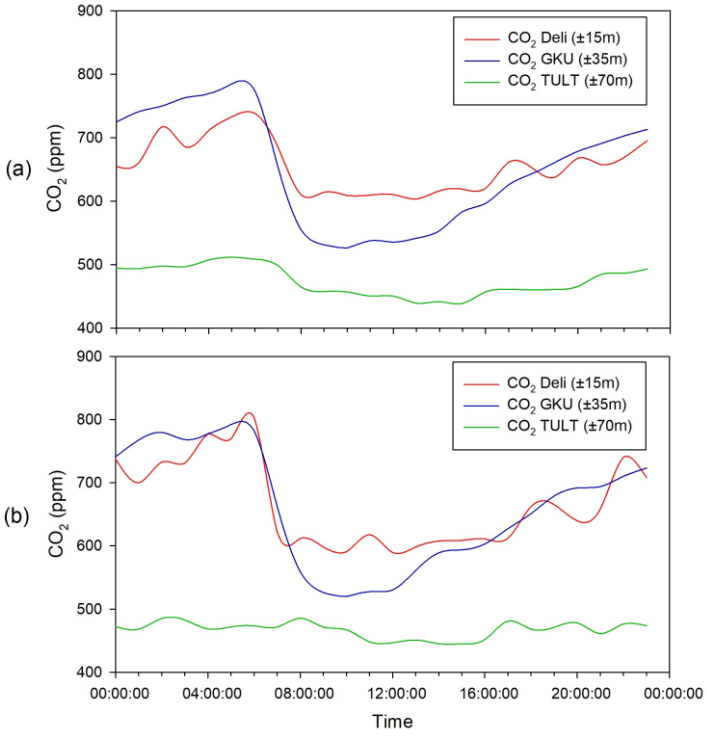

Fig. 6. Graph of CO_2 concentration during (a) weekdays and (b) weekends.

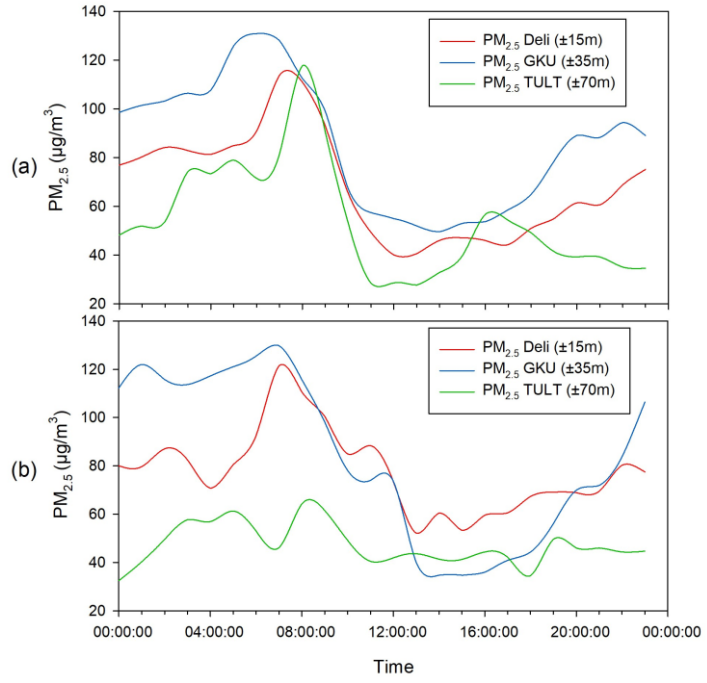

Fig. 7. Graph of $PM_{2.5}$ concentration during (a) weekdays and (b) weekends.

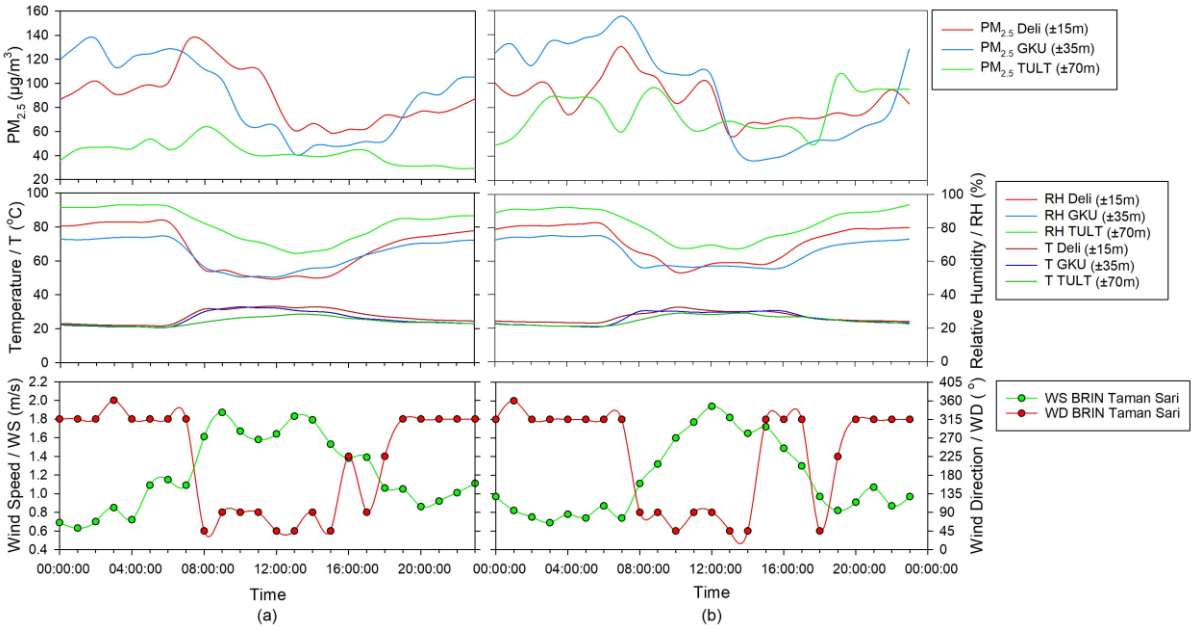

Fig. 8. Graph of $PM_{2.5}$ concentration and meteorological parameters on (a) Saturday and (b) Sunday.

3.2 Horizontal Analysis

The horizontal review used an independent T-test / One-way ANOVA to test for homogeneity and heterogeneity. Horizontal measurement data were taken from three stations: GKU, BRIN Pasteur, and BRIN Taman Sari. As seen in Fig. 9, the concentration of $PM_{2.5}$ in GKU from June to late July continued to increase. After further investigation, it was found that there were nearby emissions, specifically on Radio Street, which is currently the location of a construction project. After being interviewed, The project began excavation at the end of June and is aimed at constructing a new campus. Emissions from the project are primarily generated by building materials and a continuous influx of large vehicles. This indicates why from the end of June until now, the concentration of $PM_{2.5}$ has increased significantly.

After that, the next step is to analyze the Spatiotemporal homogeneity and heterogeneity. `In the brown box week, the data trend is relatively the same between one station and another. During the measurement in the brown box, the cardinal directions always point to the dominant direction. After being tested using an independent T-test / One-way ANOVA, the data in the brown box has a homogeneous value, or it can be said that there is no significant difference. In contrast, the blue box shows that in the measurement, one station has a different trend from other stations. This is due to solid local emissions that only occur at that station and cannot be read at other stations. According to the authors' research, an anomaly at the station occurs when the cardinal directions on that day are not in the same direction as the dominant cardinal directions.

Then, for the value of CO_2 concentration, after an independent T-test / One-way ANOVA test is carried out, the significance value is found in the gray box in Fig. 10. Differences in CO_2 concentration are noticeable. Homogeneity is observed only in the early weeks of June. For the rest of the time, there is a significant difference between one station and another, resulting in heterogeneous values for the three data sets. This can be determined by the significance value, which is less than 0.05. These differences are attributed to the characteristics of the measurement sites.

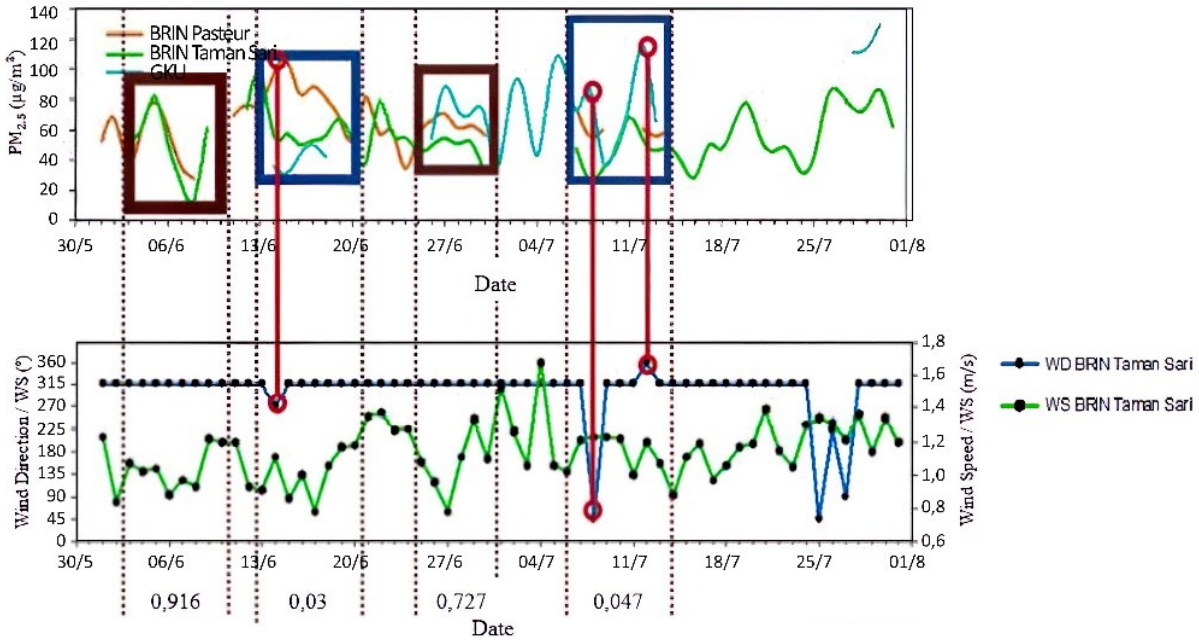

Fig. 9. $PM_{2.5}$ Homogeneity test data and results.

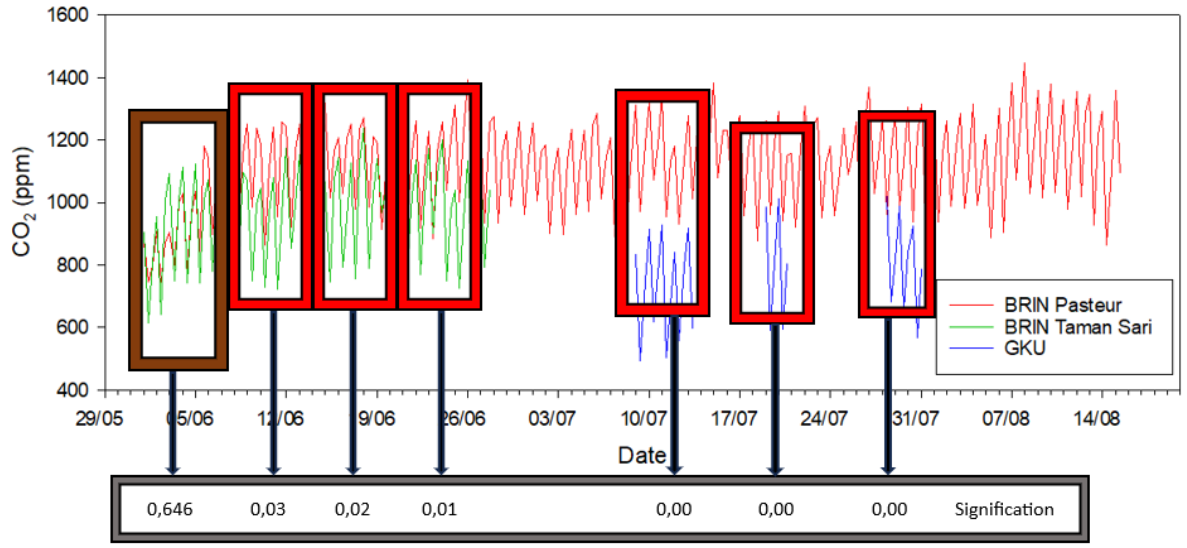

Fig. 10. CO_2 homogeneity test data and results.

It can be seen from the location in Fig. 11 that each monitoring location has its characteristics at BRIN Pasteur. Several plants around it have the function of reducing CO_2 gas during the day, but this monitoring location is right next to the main road, so it affects the CO_2 concentration. In contrast to BRIN Pasteur, the measurement area for BRIN Taman Sari contains over 80% green open space, which has an impact on the lower CO_2 concentration.

During the day, CO_2 reaches the lowest point of ±600 ppm. However, the value is still high because of tourist attractions, such as a zoo, and adjacent to a busy road. While the GKU has a relatively low value, at the GKU measurement station, several green open spaces contribute to CO_2 reduction. Also, the monitoring location is quite far from the main road.

(a) (b) (c)

Fig. 11. Location of measuring instrument installation. (a) BRIN Pasteur, (b) BRIN Taman Sari, and (c) GKU (Telkom University).

3.3 Long-distance Pollution Transport

A backward trajectory calculation was carried out using HYSPLIT [29] to determine the characteristics of the transport path and the estimation of long-distance $PM_{2.5}$ sources. HYSPLIT models replicate the dispersion and path of substances as they are transported and dispersed across different scales, from local to global, within the Earth's atmosphere. The concentrations of air pollutants are determined for individual grid cells, considering both advection and diffusion. The movement and dispersion of particles are calculated based on their starting positions [30]. The backward trajectory calculation was conducted from 2019 to 2020, encompassing multiple seasons to capture their respective characteristics. Since the measurements were conducted during the dry season, the backward trajectory data was obtained specifically for that season to illustrate the direction of air parcel trajectories in accordance with the monsoon wind cycle.

Furthermore, grouping is carried out based on the spatial and temporal distribution of air parcel paths using a clustering algorithm where the method used is angle distance. There are 6 clusters of trajectories each season. The pollution cluster is determined, namely the cluster of trajectories that are considered the main routes that play a role in long-distance $PM_{2.5}$ transportation. Pollution clusters are identified when the number of pollution paths within the cluster exceeds one-sixth of the total pollution trajectories for a season. The pollution trajectory is the air parcel trajectory when the measured $PM_{2.5}$ exceeds the 55 $\mu g/m^3$ threshold. The result is a map per trajectory cluster can be seen in Fig. 12.

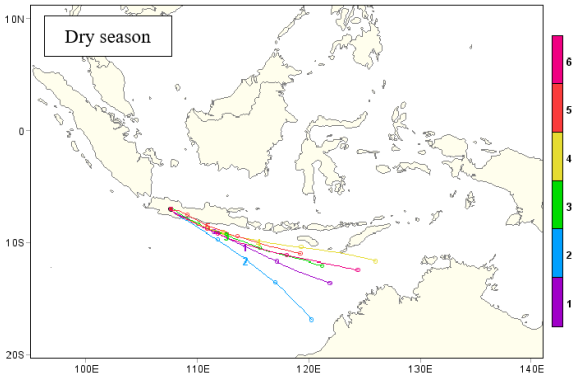

Fig. 12. Results of trajectory clustering in the Dry Season.

Table 1. Cluster Analysis in Dry Season.

Cluster	All Trajectory			Pollution Trajectory		
	Total Trajectory of The Cluster (%)	$PM_{2.5}$ Average ($\mu g/m^3$)	Std. Dev.	Total Cluster Pollution Trajectory (%)	Average $PM_{2.5}$ Pollution Trajectory ($\mu g/m^3$)	Std. Dev.
1	18.75	35.63	23.44	20.87	72.89	19.44
2	17.26	31.33	22.90	12.60	80.56	19.23
3	13.28	28.61	16.18	5.51	67.60	15.60
4	15.64	36.19	28.74	22.44	79.04	21.28
5	6.41	57.05	39.19	13.78	94.19	41.79
6	28.66	31.89	25.37	24.80	81.90	23.68
Total		34.34	26.07		80.11	25.61

Backward trajectory analysis with clustering effectively shows the characteristics of the transport trajectory $PM_{2.5}$ but cannot display the potential source area. In addition, the analysis also has weaknesses where the results depend on the method chosen [24, 31]. A long-distance pollutant is calculated as a potential source contribution function (PSCF) to estimate the potential source area. The representation on the map is then divided based on the PSCF value, with the color: blue for values 0.1 – 0.2;

light blue for values 0.2 – 0.3; green for values 0.3 – 0.4; yellow for values 0.4 – 0.5; orange for values 0.5 – 0.6; red for values 0.6 – 0.7; and purple for the value of 0.7. An area with an enormous PSCF value indicates a high probability of being a potential source of pollutant distance away [23].

It can be seen in Fig. 13 that overall, the majority of PSCF values are low at 0.2-0.5. This could be due to the $PM_{2.5}$ concentration in this season, which is generally below the threshold. However, there are areas with a PSCF value of 0.7 in the northern part of West Java, precisely in the Cirebon area, an urban area, and a sea transportation stopover route. PSCF values of 0.5-0.6 with small coverage are also found in the southern regions of East Java and the Indian Ocean.

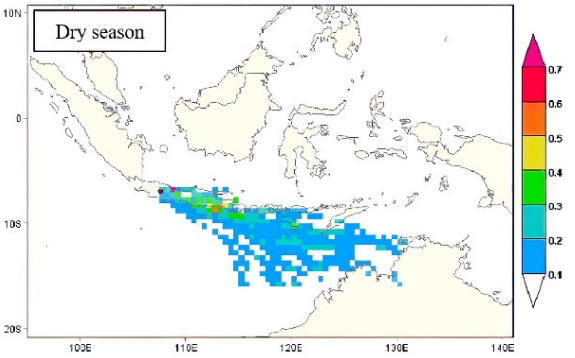

Fig. 13. PSCF results on Dry Season.

PSCF cannot show the contribution of potential source areas quantitatively. In addition, the calculation considers a much higher $PM_{2.5}$ concentration value to be slightly higher than the threshold [24]. For this reason, a Concentration Weight Trajectory (CWT) calculation is carried out to support the PSCF analysis. The results of the CWT calculation show the average concentration of the $PM_{2.5}$ potential source area based on a backward trajectory. The value shown is not the actual concentration value of the area. However, it can describe the area's contribution level relative to the measured $PM_{2.5}$ concentration [23, 26].

The CWT results show a similar picture to the PSCF results Fig. 14. Orange-colored areas to the purple are considered the main contributor areas. In the dry season, the main contributor areas are the Indian Ocean, the Cirebon City, and the West Java – Central Java border, with a $PM_{2.5}$ load of 55 – 65 $\mu g/m^3$. The potential source area resulting from CWT calculations is slightly broader than that from PSCF calculations because CWT considers the entire backward trajectory. In the ocean, the pollutants can be caused by the activity of phytoplankton and algae, marine transportation, and sea salt aerosols [32]. It is known from previous research that there is a salt content that is not a local pollutant and sulfate, which may come from sea transportation in particulates [33, 34].

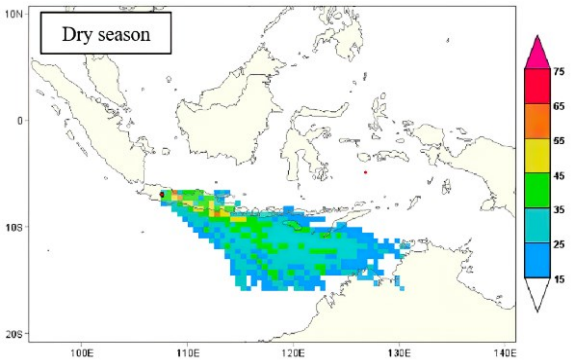

Fig. 14. CWT results in Dry Season.

4. Conclusions

In the vertical view, the CO_2 concentration at the TULT measuring station is no longer directly affected by CO_2 emissions from local activities seen from the trend of the data, which is relatively in the range of 450-500 ppm without the influence of day and night changes. $PM_{2.5}$ concentrations on weekends are relatively low by range around 35-70 $\mu g/m^3$ and are less affected by changes in day and night. However, on weekdays there is still an increase in $PM_{2.5}$ concentration which is influenced by local activities with concentrations that tend to be lower than the other two measuring stations.

Then from the results of horizontal measurements after testing homogeneity or heterogeneity, $PM_{2.5}$ significance was obtained with a significance value of more than 0.05. It shows that $PM_{2.5}$ concentrations tend to be homogeneous, except when an anomaly occurs, such as the cardinal directions opposite the dominant cardinal directions from 13 to June 20, 2022, and 7 to July 14, 2022. Whereas for CO_2 during monitoring and data validation, homogeneous values only occurred from early June 1 to June 07, 2022. The rest had significant or heterogeneous differences, and this was due to the different characteristics of each measurement station and the influence of open space. The green area is different from each station, so for CO_2, the effect or spatial characteristics of the measuring station area determine its concentration.

The vertical and horizontal analysis shows that CO_2 concentrations tend to be heterogeneous due to differences in altitude and spatial characteristics of the measurement sites. Meanwhile, $PM_{2.5}$ tends to be more homogeneous by having the same pattern at different heights and spatial locations, even though it has different concentrations at each measurement station. For the long-distance pollution potential, the PSCF and CWT results on the backward trajectory show that the estimated long-distance $PM_{2.5}$ potential

source area is from the Indian Ocean and Cirebon area, which has a high PSCF and CWT value. This area has a high contribution during the dry season, with $PM_{2.5}$ loads of 55 - 65 μg/m^3. This result indicates that the site is a potential long-range $PM_{2.5}$ source.

Acknowledgment

This work is partially supported by PT. Eskhalasi Langit Biru and Telkom University, Indonesia.

References

[1] A. K. Gorai, P. B. Tchounwou, S. S. Biswal, and F. Tuluri, "Spatio-Temporal Variation of Particulate Matter(PM2.5) Concentrations and Its Health Impacts in a Mega City, Delhi in India," *Environ Health Insights*, vol. 12, 2018, doi: 10.1177/1178630218792861.

[2] "Peraturan Pemerintah Republik Indonesia Nomor 22 Tahun 2021 Tentang Penyelenggaraan Perlindungan dan Pengelolaan Lingkungan Hidup," 2021.

[3] World Health Organization, "Ambient air pollution attributable deaths," Jul. 06, 2018. https://www.who.int/data/gho/data/indicators/indicator-details/GHO/ambient-air-pollution-attributable-deaths (accessed Dec. 05, 2021).

[4] M. Santoso *et al.*, "Long term airborne lead pollution monitoring in Bandung, Indonesia," *International Journal of PIXE*, vol. 24, no. 03n04, pp. 151–159, Jan. 2014, doi: 10.1142/s0129083514400087.

[5] "Jumlah penduduk dan laju pertumbuhan penduduk di kota bandung 2011-2016," *Badan Pusat Statistik*. https://bandungkota.bps.go.id/statictable/2017/08/29/106/-jumlah-penduduk-dan-laju-pertumbuhan-penduduk-di-kota-bandung-2011---2016-.html (accessed Jul. 18, 2023).

[6] "Badan Pusat Statistik Kota Bandung." https://bandungkota.bps.go.id/ (accessed Apr. 20, 2021).

[7] D. R. Peters et al., "Evaluating uncertainty in sensor networks for urban air pollution insights," Atmos Meas Tech, vol. 15, no. 2, pp. 321–334, Jan. 2022, doi: 10.5194/amt-15-321-2022.

[8] "Data Online Pusat Database - BMKG." http://dataonline.bmkg.go.id/ (accessed Aug. 21, 2022).

[9] A. H. Mustofa, I. Chandra, and R. A. Salam, "Pengukuran Konsentrasi PM2.5 dan CO2 Pada Struktur Vertikal Cekungan Udara Bandung Raya." 2020.

[10] F. W. Lurmann, A. S. Wexler, S. N. Pandis, S. Musarra, N. Kumar, and J. H. Seinfeld, "Modelling urban and regional aerosols—II. Application to California's South Coast Air Basin," *Atmos Environ*, vol. 31, no. 17, pp. 2695–2715, Sep. 1997, doi: 10.1016/S1352-2310(97)00100-3.

[11] R. Zalakeviciute, J. López-Villada, and Y. Rybarczyk, "Contrasted effects of relative humidity and precipitation on urban PM2.5 pollution in high elevation urban areas," *Sustainability (Switzerland)*, vol. 10, no. 6, Jun. 2018, doi: 10.3390/su10062064.

[12] Y. Li, Q. Chen, H. Zhao, L. Wang, and R. Tao, "Variations in PM10, PM2.5 and PM1.0 in an Urban Area of the Sichuan Basin and Their Relation to Meteorological Factors," *Atmosphere (Basel)*, vol. 6, no. 1, pp. 150–163, Jan. 2015, doi: 10.3390/atmos6010150.

[13] J. Wang and S. Ogawa, "Effects of Meteorological Conditions on PM2.5 Concentrations in Nagasaki, Japan," *Int J Environ Res Public Health*, vol. 12, no. 8, pp. 9089–9101, Aug. 2015, doi: 10.3390/ijerph120809089.

[14] F. Zhang *et al.*, "Fine particles (PM2.5) at a CAWNET background site in Central China: Chemical compositions, seasonal variations and regional pollution events," *Atmos Environ*, vol. 86, pp. 193–202, Apr. 2014, doi: 10.1016/j.atmosenv.2013.12.008.

[15] X. Y. Ni, H. Huang, and W. P. Du, "Relevance analysis and short-term prediction of PM 2.5 concentrations in Beijing based on multi-source data," *Atmos Environ*, vol. 150, pp. 146–161, Feb. 2017, doi: 10.1016/j.atmosenv.2016.11.054.

[16] R. Jayamurugan, B. Kumaravel, S. Palanivelraja, and M. P. Chockalingam, "Influence of Temperature, Relative Humidity and Seasonal Variability on Ambient Air Quality in a Coastal Urban Area," *International Journal of Atmospheric Sciences*, vol. 2013, pp. 1–7, Dec. 2013, doi: 10.1155/2013/264046.

[17] A. Sya'bani *et al.*, "Pemantauan Konsentrasi PM2.5 dan CO2 Berbasis Low-Cost Sensor secara Real-Time di Cekungan Udara Bandung Raya," *Jurnal Teknologi Lingkungan*, vol. 21, no. 1, pp. 9–15, Jan. 2020, doi: 10.29122/jtl.v21i1.3707.

[18] "Household air pollution and health," *WHO*. https://www.who.int/en/news-room/fact-sheets/detail/householdair-pollution-and-health (accessed Oct. 03, 2021).

[19] F. Vaicdan, I. Chandra, and A. Suhendi, "Pengamatan Konsentrasi Massa PM2.5 di Cekungan Udara Bandung Raya," 2019.

[20] P. Mishra, U. Singh, C. Pandey, P. Mishra, and G. Pandey, "Application of student's t-test, analysis of variance, and covariance," *Ann Card Anaesth*, vol. 22, no. 4, p. 407, 2019, doi: 10.4103/aca.ACA_94_19.

[21] M. Alassaf and A. M. Qamar, "Improving Sentiment Analysis of Arabic Tweets by One-

way ANOVA," *Journal of King Saud University - Computer and Information Sciences*, vol. 34, no. 6, pp. 2849–2859, Jun. 2022, doi: 10.1016/j.jksuci.2020.10.023.
[22]M. Bildirici and S. M. Gokmenoglu, "The impact of terrorism and FDI on environmental pollution: Evidence from Afghanistan, Iraq, Nigeria, Pakistan, Philippines, Syria, Somalia, Thailand and Yemen," *Environ Impact Assess Rev*, vol. 81, p. 106340, Mar. 2020, doi: 10.1016/j.eiar.2019.106340.
[23]A. Stohl, "Computation, accuracy and applications of trajectories—A review and bibliography," *Atmos Environ*, vol. 32, no. 6, pp. 947–966, Mar. 1998, doi: 10.1016/S1352-2310(97)00457-3.
[24]C. Li, Z. Dai, X. Liu, and P. Wu, "Transport Pathways and Potential Source Region Contributions of PM2.5 in Weifang: Seasonal Variations," *Applied Sciences*, vol. 10, no. 8, p. 2835, Apr. 2020, doi: 10.3390/app10082835.
[25]H. Li, Q. He, and X. Liu, "Identification of Long-Range Transport Pathways and Potential Source Regions of PM2.5 and PM10 at Akedala Station, Central Asia," *Atmosphere (Basel)*, vol. 11, no. 11, p. 1183, Nov. 2020, doi: 10.3390/atmos11111183.
[26]T. Hao, Z. Cai, S. Chen, S. Han, Q. Yao, and W. Fan, "Transport Pathways and Potential Source Regions of PM2.5 on the West Coast of Bohai Bay during 2009–2018," *Atmosphere (Basel)*, vol. 10, no. 6, p. 345, Jun. 2019, doi: 10.3390/atmos10060345.
[27]Y. W. Utama, "Distribusi Temporal Konsentrasi PM10 Menggunakan Alat Particle Plus EM-10000," *Ecolab*, vol. 15, no. 1, pp. 45–52, May 2021, doi: 10.20886/jklh.2021.15.1.45-52.
[28]Y. Li, J. Deng, C. Mu, Z. Xing, and K. Du, "Vertical distribution of CO2 in the atmospheric boundary layer: Characteristics and impact of meteorological variables," *Atmos Environ*, vol. 91, pp. 110–117, 2014, doi: 10.1016/j.atmosenv.2014.03.067.
[29]"HYSPLIT," *NOAA Air Resources Laboratory*. https://www.ready.noaa.gov/HYSPLIT.php (accessed Jul. 18, 2023).
[30]Q. Wang, T. Zhao, R. Wang, and L. Zhang, "Backward Trajectory and Multifractal Analysis of Air Pollution in Zhengzhou Region of China," *Math Probl Eng*, vol. 2022, pp. 1–17, Jan. 2022, doi: 10.1155/2022/2226565.
[31]L. Cui, X. Song, and G. Zhong, "Comparative Analysis of Three Methods for HYSPLIT Atmospheric Trajectories Clustering," *Atmosphere (Basel)*, vol. 12, no. 6, p. 698, May 2021, doi: 10.3390/atmos12060698.
[32]M. Rinaldi *et al.*, "Primary and Secondary Organic Marine Aerosol and Oceanic Biological Activity: Recent Results and New Perspectives for Future Studies," *Advances in Meteorology*, vol. 2010, pp. 1–10, 2010, doi: 10.1155/2010/310682.
[33]L. I. Majid, I. Chandra, A. Rohsari, and I. Utami, "Observasi Lapangan Mikro-partikel di Atmosfer Menggunakan Nanosampler Pada Cekungan Udara Bandung Raya." Apr. 2019.
[34]R. Adam, A. Barus, I. Chandra, and I. W. Fathona, "Rancang Bangun Portable Weather Station Dalam Mendukung Pengamatan Mikropartikel di Cekungan Udara Bandung Raya." Apr. 2019.

Author information

Indra Chandra took his undergraduate education at Bandung Institute of Technology in 2000, majoring in physics and instrumentation. Then in 2004 took a master's education at the same university and major. Then, in 2014 he took his doctorate at Kanazawa University, majoring in Instrumentation, Environment, Science, and Atmospheric Technology. Has been a Director at the Sandhy Putra Telecommunication Engineering Academy from 2020-2021. While working at Telkom University, he was a special staff to the Chancellor in 2010-2011. Became Head of Engineering Physics Study Program in 2012-2014. In addition, he became Assistant Professor in 2008 until now.

Rahmat Awaludin Salam took his undergraduate education at the Indonesian University of Education in 2006, majoring in Physics. Then, in 2011 he took his master's education at the Bandung Institute of Technology majoring in Physics and his doctoral education in 2013 with the same university and major.

Andre Suwardana Adiwidya took his undergraduate education at Telkom University in 2018, majoring in engineering physics. Became a mechatronics lab assistant in 2020 and automatic control practicum

assistant in 2021. He graduated with a bachelor's degree in 2022 and continued his master's education at Telkom University in 2023 with a major in Electrical Engineering.

.

Reza Mochamad Aziz took undergraduate education at Telkom University in 2018, majoring in engineering physics. Became an Electronic and Intelligence Robotics Research Group lab assistant in 2020 and automatic control practicum assistant in 2021.

Mohammad Beno Afryan took his undergraduate education at Telkom University in 2016, majoring in engineering physics. Research in his final assignment is about estimating the potential source of $PM_{2.5}$ using a backward trajectory and the Potential Source Contribution Factor (PSCF) method.

Tania Christiana Alexandra is an undergraduate in Engineering Physics at Telkom University 2019 with a GPA of 3.95. Active in various activities, such as programming assistant for 2 years from 2020-2022 in the Basic Computing Laboratory and practicum assistant of signal processing in 2022. In addition, as the team leader, she succeeded in becoming the top 5 Finalist for YESIST12 IEEE 2022 Innovation Challenge Track Indonesia Pilot with the title "WARMs for DRR: Water and Air Real-Time Monitoring System for Disaster Risk Reduction due to Greenhouse Gases." Has experience in leadership, product strategy, education, and programming.

Mario Gilang Permadi is an undergraduate student at Telkom University in 2020, majoring in Engineering Physics. He joined as a lab assistant in the Thermal Analysis Laboratory. He also had an internship in a research lab, namely Atmospheric Environment Laboratory.

Nur Rawdotul Jannah is a 2020 Physics Engineering undergraduate student at Telkom University. Become an assistant in the Instrumentation Systems Laboratory in 2022 and a research assistant in the Biospin Laboratory in 2022. She also has teaching experience by joining as a lecturer on the Superprof platform in physics and mathematics. In addition, she was a finalist at the international level in the Biomedical Engineering Smart Exhibition at the Biomedical Engineering Annual Contest held by the Biomedical Engineering Department of ITS.

Dini Rizqi Amalia is a Telkom University 2020 student in Physics Engineering major. She has been a practicum assistant at Basic Computer Laboratory since 2021, which helps TPB students to learn about basic C programming.

Nur Putri Megalia is an undergraduate student at Telkom University in 2020, majoring in Engineering Physics. Become an Instrumentation System Laboratory assistant in 2022 and research assistant in a Biomedical Signal Processing and Instrumentation laboratory in 2022.

Vivian Lee is an undergraduate student at Telkom University in 2020, majoring in Engineering Physics. She has participated in several competitions, including the Top 120 "Innovillage 2020". Being an assistant in the Engineering Thermodynamics laboratory and an intern at the Atmospheric Environment Laboratory.

Additional Information